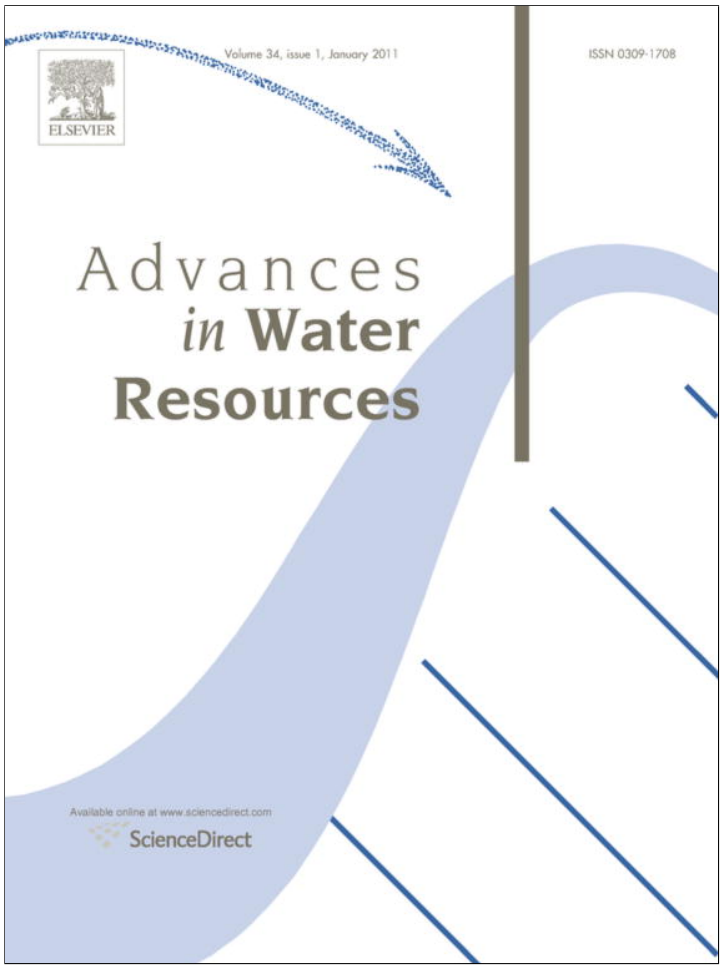

(This is a sample cover image for this issue. The actual cover is not yet available at this time.)

Advances in Water Resources 34 (2011) 1681–1693

Contents lists available at SciVerse ScienceDirect

Advances in Water Resources

journal homepage: www.elsevier.com/locate/advwatres

Effect of fracture pressure depletion regimes on the dual-porosity shape factor for flow of compressible fluids in fractured porous media

Ehsan Ranjbar, Hassan Hassanzadeh *, Zhangxin Chen

Department of Chemical and Petroleum Engineering, Schulich School of Engineering, University of Calgary, 2500 University Drive N.W., Calgary, Alberta, Canada T2N 1N4

ARTICLE INFO

Article history:
Received 16 April 2011
Received in revised form 22 September 2011
Accepted 26 September 2011
Available online 1 October 2011

Keywords:
Matrix-fracture boundary conditions
Shape factor
Variable fracture pressure
Compressible fluids
Dual-porosity systems
Single-phase flow

ABSTRACT

A precise value of the matrix-fracture transfer shape factor is essential for modeling fluid flow in fractured porous media by a dual-porosity approach. The slightly compressible fluid shape factor has been widely investigated in the literature. In a recent study, we have developed a transfer function for flow of a compressible fluid using a constant fracture pressure boundary condition [Ranjbar E, Hassanzadeh H, Matrix-fracture transfer shape factor for modeling flow of a compressible fluid in dual-porosity media. Adv Water Res 2011;34(5):627–39. doi:10.1016/j.advwatres.2011.02.012]. However, for a compressible fluid, the consequence of a pressure depletion boundary condition on the shape factor has not been investigated in the previous studies. The main purpose of this paper is, therefore, to investigate the effect of the fracture pressure depletion regime on the shape factor for single-phase flow of a compressible fluid. In the current study, a model for evaluation of the shape factor is derived using solutions of a nonlinear diffusivity equation subject to different pressure depletion regimes. A combination of the heat integral method, the method of moments and Duhamel's theorem is used to solve this nonlinear equation. The developed solution is validated by fine-grid numerical simulations. The presented model can recover the shape factor of slightly compressible fluids reported in the literature. This study demonstrates that in the case of a single-phase flow of compressible fluid, the shape factor is a function of the imposed boundary condition in the fracture and its variability with time. It is shown that such dependence can be described by an exponentially declining fracture pressure with different decline exponents. These findings improve our understanding of fluid flow in fractured porous media.

1. Introduction

In general, there are computational challenges in upscaling of fluid flow in fractured formations. Upscaling of transport and flow parameters for porous media has been investigated from decades and a range of upscaling techniques have been introduced [1]. Large portion of the produced natural gas occurs from fractured formations including naturally fractured reservoirs (NFR), coal bed methane (CBM) and tight fractured gas reservoirs. In these reservoirs, the major storage for the reservoir fluids is in the matrix whereas flow primarily occurs in the highly conductive fractures [2]. Warren and Root [3] established the dual-porosity model for modeling of a slightly compressible fluid flow in the naturally fractured reservoirs. In the dual-porosity approach, a fractured reservoir is divided into two media with completely different properties: fracture and matrix. The fracture network supplies the main flow paths and the reservoir rock or matrix acts as the major source of the fluid storage [4]. On the other hand most of the fluid storage is in the matrix and fluid flows through the fractures as the main channel. Therefore, an improved dual porosity model should be able to accurately account for the fracture and matrix interaction.

A dual-porosity model, which is an effective and broadly used approach for modeling and upscaling of fluid flow in the fractured porous media, assumes that two distinct types of porosity coexist in a representative rock volume [2,5–8]. In general, fracture has a low storage capacity and high transmissivity and the adjacent rock matrix has a high storage capacity and a relatively low transmissivity [9]. Defining the transfer shape factor that accounts for the interaction among the matrix and fracture is a great challenge in dual-porosity upscaling. In dual-porosity models the matrix-fracture interaction is modeled through a shape factor. An equivalent fracture permeability, matrix-permeability, matrix-fracture transfer coefficient (shape factor) and saturation functions (for multiphase flow) are essential parameters for the dual porosity approach. Studies have been conducted in the past to determine the transfer shape factor for slightly compressible fluids in the fractured reservoirs [10–17]. A precise value of the shape factor is essential to consider transient and pseudo-steady state performance of the matrix-fracture interaction and also geometry of

* Corresponding author. Tel.: +1 403 210 6645; fax: +1 403 284 4852.
E-mail address: hhassanz@ucalgary.ca (H. Hassanzadeh).

0309-1708/$ - see front matter © 2011 Elsevier Ltd. All rights reserved.
doi:10.1016/j.advwatres.2011.09.010

Nomenclature

A	cross-sectional area [L^2]
B_g	gas formation volume factor
c_m	matrix total compressibility [LT^2/M]
$h_m = 2L_c$	matrix block length [L]
k_m	matrix permeability [L^2]
l	time dependent length where pressure is average pressure [L]
L_c	matrix block characteristic length [L]
n	exponent in the polynomial trial solution using HBIM
p_m	matrix-block pressure [M/LT^2]
$\bar{p}_m$	average matrix-block pressure [M/LT^2]
p_f	fracture pressure [M/LT^2]
q_{sc}	matrix-fracture fluid transfer [L^3/T]
$\hat{q}$	interporosity flow rate per unit volume of rock [$1/T$]
t	time [T]
t^*	dimensionless time at which the pressure disturbance reach to the boundary
t_D	dimensionless time
T	reservoir temperature [K]
V_b	matrix-block volume [L^3]
x_D	dimensionless distance

Greek Symbols

α	decline constant [$1/T$]
β	space correction factor
γ	gas specific gravity
δ	penetration depth
ε	proportionality constant for penetration depth
η_m	matrix hydraulic diffusivity [L^2/T]
$\bar{\eta}$	average hydraulic diffusivity [L^2/T]
η_D	dimensionless hydraulic diffusivity
η_{D1}	dimensionless fracture hydraulic diffusivity
κ	dimensionless decline constant
λ	dimensionless exponent of solution of gas diffusivity equation using moment method
μ	fluid viscosity [M/LT]
σ	shape factor [$1/L^2$]
τ	Duhamel 's variable
ϕ	porosity
$\bar{\psi}_m$	average matrix-block pseudo-pressure [M/LT^3]
ψ_f	fracture pseudo-pressure [M/LT^3]
ψ_i	initial pseudo-pressure [M/LT^3]
ψ_D	dimensionless pseudo-pressure
ψ_{fD}	dimensionless fracture pseudo-pressure
$\bar{\psi}_D$	average dimensionless pseudo-pressure
ψ_∞	fracture pseudo-pressure when t_D tends to infinity [M/LT^3]

Subscripts

D	dimensionless
f	fracture
g	gas
i	initial condition
m	matrix
SC	standard conditions

the matrix-fracture system. It should be noted that the functionality of the fracture pressure as a boundary to the matrix blocks may also have a significant effect on the stabilized value of the shape factor for a slightly compressible fluid [18,19].

In traditional dual porosity formulation the flow between the matrix and the fracture is considered by a transfer function, which acts as a source term in the governing equation for fluid flow in the fractures. Darcy's law is used in this source function over the mean path between the matrix and the adjacent fracture. In the non-coupled dual porosity formulation, flow in the fractures acts as a boundary condition for flow in the matrix [9]. This transfer function and the amount of fluid that is transferred from the matrix to the fracture are directly proportional to the shape factor. Numerical simulation of naturally fractured reservoirs using a dual porosity approach requires a precise value of the shape factor for the entire period of the production time.

In general, there are two models to consider the matrix and fracture interaction including pseudo-steady state and transient transfer. The former model ignores the pressure transient in the matrix while the latter model accounts for the pressure transient in the matrix. The matrix-fracture shape factor for a slightly compressible fluid can be obtained using the following equation [20]:

$$\sigma = -\frac{\mu c_m \phi_m}{k_m} \frac{\frac{\partial \bar{p}_m}{\partial t}}{(\bar{p}_m - p_f)}, \tag{1}$$

where μ is the fluid viscosity, c_m, ϕ_m, and k_m are the total isothermal compressibility, porosity and permeability, respectively, $\bar{p}_m$ shows the average pressure of the matrix block, p_f is the fracture pressure and σ is the matrix-fracture transfer shape factor with dimension of L^{-2}. In a pseudo-steady state model the matrix blocks are considered as a lumped system with an average pressure, $\bar{p}_m$, while in the transient model one needs to find the solution of the pressure diffusivity equation given by:

$$\nabla\left(\frac{k_m}{\mu}\nabla p_m\right) = \phi_m c_m \frac{\partial p_m}{\partial t}. \tag{2}$$

For a slightly compressible fluid, negligible variation of the fluid viscosity and isothermal compressibility with the pressure leads to a linear flow equation for the pressure variation in the matrix. This equation can be solved by common analytical or semi-analytical methods such as the Laplace transform or separation of variables method [8,20–23].

Determination of the matrix-fracture transfer shape factor for a slightly compressible fluid based on the pseudo-steady state or transient transfer model has been studied in the past. Investigators have considered the effect of fracture boundary conditions on the dual porosity formulation and shape factor for the slightly compressible fluids [18,19,24]. It has been shown that the fracture pressure and its variation with time affect the transient and pseudo-steady state values of the shape factor.

There have been new efforts to determine the shape factors for multi-phase flow and thermal methods in fractured porous media [24–26]. There have also been a few reports in the literature to model dual porosity systems for compressible fluids with different approaches than this study [27,28]. A more detailed review of shape factor developments was discussed elsewhere [29].

Although the dual porosity approach with the shape factor concept has some limitations, it has been widely used and well accepted approach in hydrological sciences and petroleum reservoir modeling. This may be because of its simplicity, computational efficiency and flexibility in application to various fluid flow and transport problems. In addition, lack of more advanced and efficient models that can accurately take into account the matrix-fracture interaction have contributed to extensive use of the dual porosity models. Currently, the majority of commercial flow simulators use the dual porosity approach. However, it should be

pointed out that a new line of attack on tackling fluid flow and transport in fractured rocks has been recently introduced based on discrete fracture network models [30]. Hoteit and Firoozabadi [30] presented a discrete fracture model for single phase flow of compressible fluids in heterogeneous and fractured media. They developed a numerical model by combining the mixed finite element and the discontinuous Galerkin methods for multi-component gas flow. Discrete fracture model also have been used for multiphase flow and water injection in fractured media [31,32].

It has been reported in the literature that in the case of a slightly compressible fluid the pseudo-steady state value of the matrix-fracture shape factor is a function of the pressure decline regime in the fracture. Contrary to the slightly compressible fluid case, the variation of the isothermal compressibility and viscosity with pressure cannot be ignored when dealing with a compressible fluid. This leads to a nonlinear PDE. Therefore, the reported shape factors for slightly compressible fluids cannot be applied for compressible fluids or their application has not been validated in the previous studies. In a recent study we derived the matrix-fracture shape factor for a compressible fluid in dual-porosity systems [29]. The effect of fracture pressure decline on the compressible fluid shape factor has not been reported in the previous studies. In this study, we further develop our previous study to investigate the effect of pressure decline in the fracture on the matrix-fracture transfer shape factor for a compressible fluid.

We study the influence of the fracture pressure (as a boundary condition for the matrix block) on the shape factor for flow of a compressible fluid in a dual-porosity model which has not been investigated in the former works. To obtain the matrix-fracture shape factor, a nonlinear diffusivity equation is solved using the heat integral method and the method of moments. To consider the effect of the time variation of the boundary conditions a modified trial solution (early time) and Duhamel's theorem (late time) are used to derive the early and late time shape factors for the declining fracture pressure cases. The developed approximate analytical solution is validated by a numerical model [29]. The developed shape factor model can recover predictions from the shape factor models available in the literature for a slightly compressible fluid. This shape factor may find applications in dual-porosity modeling of the convectional and unconventional naturally fractured gas reservoirs such as coalbed methane and fractured tight gas reservoirs.

This paper is organized in a manner that follows a methodology for derivation of the shape factor for compressible fluids. Next solution of the nonlinear diffusivity equation subject to a declining fracture pressure is obtained using the heat integral and moment methods and Duhamel's theorem. Afterwards model verification and results are discussed followed by conclusions.

2. Methodology

In this section the shape factor for flow of a compressible fluid from a matrix block under different fracture boundary conditions is derived by taking into account the pressure dependency of the viscosity and isothermal compressibility. Darcy's law for flow of gas in the porous media is expressed as follows:

$$q_{gsc} = -\frac{k_m A}{\mu B_g}\frac{dp}{dx}, \tag{3}$$

where A is the cross-section area and B_g is the gas formation volume factor. Using the definitions of the gas formation volume factor and real gas pseudo-pressure [34] and writing the Darcy's law over some characteristics length l, leads to the following equation:

$$q_{sc} = \frac{k_m T_{sc}}{T p_{sc}}\frac{A}{l}\frac{\bar{\psi}_m - \psi_f}{2}. \tag{4}$$

As shown in Eq. (4) l is a length where the matrix pressure is equal to its average pressure and this length changes with time during transient matrix production. For a matrix-fracture combination shown in Fig. 1, Eq. (4) is multiplied and divided by the bulk volume of the matrix-block to define the transfer function for compressible fluids. Using the definition of the shape factor (Eq. (5)); the final equation for the matrix-fracture transfer function for compressible fluids (e.g. gases), is expressed as Eq. (6) [29]:

$$\sigma = \frac{A}{l(V_b/2)}, \tag{5}$$

$$q_{sc} = \frac{T_{sc} V_b}{4 p_{sc}}\frac{k_m \sigma}{T}(\bar{\psi}_m - \psi_f). \tag{6}$$

In this equation T is the absolute temperature, σ is the shape factor, $\bar{\psi}_m$ shows the average matrix block pseudo-pressure and ψ_f is the fracture pseudo-pressure.

According to the Warren and Root [3] dual-porosity model for a slightly compressible fluid, the interporosity flow rate per unit volume of the rock can be expressed in terms of the accumulation rate in the matrix as follows:

$$\hat{q} = -\phi_m c_m \frac{\partial \bar{p}_m}{\partial t}. \tag{7}$$

The interporosity flow rate for compressible fluids can be expressed as follows [29]:

$$q_{sc} = -\frac{T_{sc} V_b}{4 p_{sc}}\frac{\mu c_m \phi_m}{T}\frac{\partial \bar{\psi}_m}{\partial t}. \tag{8}$$

Combination of Eqs. (6) and (8) leads to the following equation for single-phase shape factor of compressible fluids [29]:

$$\sigma = -\frac{\mu c_m \phi_m}{k_m(\bar{\psi}_m - \psi_f)}\frac{\partial \bar{\psi}_m}{\partial t}. \tag{9}$$

There is another alternative to derive the shape factor for compressible fluids by integrating of the diffusivity equation over the matrix-block volume. This method was used by Zimmerman et al. to derive the shape factor for slightly compressible fluids and leads to Eq. (1) [23]. By integrating of the gas diffusivity equation over half of the matrix block volume we reach to the following equation,

$$\phi_m c_m \frac{\partial \bar{\psi}_m}{\partial t} = \frac{1}{V_b/2}\int \frac{k_m}{\mu}\frac{\partial}{\partial x}\left(\frac{\partial \psi_m}{\partial x}\right) A dx. \tag{10}$$

Simplification of Eq. (10) leads to the following equation:

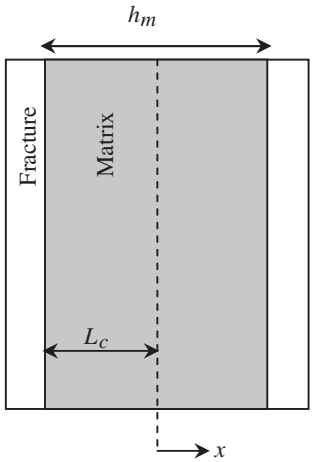

Fig. 1. Schematic of the matrix-fracture model.

$$\phi_m c_m \frac{\partial \bar{\psi}_m}{\partial t} = \frac{A}{V_b/2} \frac{k_m}{\mu} \frac{\partial \psi_m}{\partial x}. \tag{11}$$

Using the Warren and Root [3] approximation we have,

$$\frac{\partial \psi_m}{\partial x} = \frac{\psi_f - \bar{\psi}_m}{l}, \tag{12}$$

where l is the characteristics length, which is the distance from the matrix-fracture boundary where the matrix pressure is equal to its average pressure. By substituting this equation in Eq. (11) we reach to the following equation:

$$\phi_m c_m \frac{\partial \bar{\psi}_m}{\partial t} = \frac{A}{l(V_b/2)} \frac{k_m}{\mu} (\psi_f - \bar{\psi}_m). \tag{13}$$

Using the definition of the shape factor given by Eq. (5) we reach to the following equation for the shape factor of compressible fluids, which is similar to the equation that was obtained by Zimmerman et al. [23] for slightly compressible fluids. It should be noted that in this equation pseudo-pressure is appeared in the final equation as we are dealing with compressible fluids.

$$\sigma = \frac{\mu c_m \phi_m}{k_m} \frac{\frac{\partial \bar{\psi}_m}{\partial t}}{(\psi_f - \bar{\psi}_m)}. \tag{14}$$

This equation is the same as Eq. (9). It should be pointed out that for a compressible fluid the viscosity-isothermal compressibility product is a strong function of pressure, in Eq. (9) or (14) the solution of the nonlinear gas diffusivity equation is utilized to determine the shape factor for different pressure regimes in the fracture.

2.1. Constant fracture pressure

In this case it is assumed that at the matrix-fracture interface, the fracture pressure and hence the pseudo-pressure is a constant. For this case the dimensionless variables are defined as follows:

$$\psi_D = \frac{\psi_m - \psi_i}{\psi_f - \psi_i}, \tag{15}$$

$$x_D = \frac{x}{L_c}, \tag{16}$$

$$\eta_D = \frac{\eta_m}{\bar{\eta}}, \tag{17}$$

$$t_D = \frac{\bar{\eta} t}{L_c^2}. \tag{18}$$

In Eq. (17) the average hydraulic diffusivity, $\bar{\eta}$, is given by [29]:

$$\bar{\eta} = \frac{1}{p_f - p_i} \int_{p_i}^{p_f} \frac{k_m}{\mu c_m \phi_m} dp = \frac{k_m}{\phi_m} \frac{1}{p_f - p_i} \int_{p_i}^{p_f} \frac{dp}{\mu c_m}. \tag{19}$$

Using the definition of dimensionless variables (Eqs. (15), (17) and (18)) in the shape factor equation (Eq. (9)), the subsequent equation for the dimensionless shape factor in the case of the constant fracture pressure is obtained:

$$\sigma h_m^2 = -\frac{4}{\eta_D} \left(\frac{1}{\bar{\psi}_D - 1} \right) \frac{\partial \bar{\psi}_D}{\partial t_D}. \tag{20}$$

2.2. Linearly declining fracture pressure

For a linearly declining fracture pressure we have the following equation for the fracture pseudo-pressure:

$$\psi_f = \psi_i (1 - \alpha t), \quad \alpha \leqslant \frac{1}{t} \tag{21}$$

where α is a decline constant. For this case the dimensionless pseudo-pressure and the dimensionless fracture pseudo-pressure are defined as follows:

$$\psi_D = \frac{\psi_i - \psi_m}{\psi_i}, \tag{22}$$

$$\psi_{fD}(t_D) = \kappa t_D, \quad \kappa \leqslant \frac{1}{t_D} \tag{23}$$

where κ is the dimensionless decline constant and is defined as follows:

$$\kappa = \frac{\alpha t}{t_D}, \tag{24}$$

Applying the explanation of the dimensionless variables, Eqs. (17), (18), (22) and (23), in the shape factor equation (Eq. (9)), leads to the following equation for the shape factor in the case of the linearly declining fracture pressure:

$$\sigma h_m^2 = -\frac{4}{\eta_D} \left(\frac{\frac{\partial \bar{\psi}_D}{\partial t_D}}{\bar{\psi}_D - \kappa t_D} \right). \tag{25}$$

2.3. Exponentially declining fracture pressure

For this case the fracture pressure declines exponentially with time according to the following equation:

$$\psi_f = \psi_\infty + (\psi_i - \psi_\infty) \exp(-\alpha t), \tag{26}$$

where $\psi_\infty = \psi_f(t \to \infty)$. For an exponential decline, the dimensionless pseudo-pressure and the fracture dimensionless pseudo-pressure are defined as follows:

$$\psi_D(t_D) = \frac{\psi_m - \psi_i}{\psi_\infty - \psi_i}, \tag{27}$$

$$\psi_{fD}(t_D) = 1 - \exp(-\kappa t_D), \tag{28}$$

where κ is the dimensionless decline constant and is defined in Eq. (24). Using the definition of dimensionless variables (Eqs. (17), (18), (27) and (28)) in the shape factor equation (Eq. (9)), leads to the following equation for the shape factor in the case of the exponentially declining fracture pressure:

$$\sigma h_m^2 = \frac{-4}{\eta_D} \frac{\frac{\partial \bar{\psi}_D}{\partial t_D}}{\bar{\psi}_D - (1 - \exp(-\kappa t_D))}. \tag{29}$$

3. The approximate analytical solutions

The compressible fluid diffusivity equation for linear flow can be stated as:

$$\frac{\partial^2 \psi_m}{\partial x^2} = \frac{\mu c_m \phi_m}{k_m} \frac{\partial \psi_m}{\partial t}. \tag{30}$$

Strong pressure dependence of the viscosity and isothermal compressibility leads to a nonlinear partial differential equation (PDE) for compressible fluid flow in fractured porous media. Solution of this PDE cannot be obtained by common methods like Laplace or separation of variables. Eq. (30) in term of the matrix hydraulic diffusivity, $\eta_m = k_m/\mu c_m \phi_m$ is expressed as follows:

$$\frac{\partial \psi_m}{\partial t} = \eta_m(p) \frac{\partial^2 \psi_m}{\partial x^2}. \tag{31}$$

In Eq. (31), hydraulic diffusivity is a space and time dependent parameter. To solve Eq. (31), we neglect the isothermal compressibility-viscosity product variation with space and effect of the space is considered by a correction factor, β [29,33]. Fine-grid numerical simulations are used to determine this correction factor. Since the gas compressibility is orders of magnitude larger than the rock compressibility we ignore the rock compressibility in the solution [33,34]. Therefore, we reach the following PDE with the initial and boundary conditions.

$$\frac{\partial \psi_m}{\partial t} = \frac{\partial}{\partial x}\left(\beta \eta_m(t) \frac{\partial \psi_m}{\partial x}\right), \tag{32}$$

$$t = 0 \rightarrow \psi_m = \psi_i, \tag{33a}$$

$$x = 0 \rightarrow \frac{\partial \psi_m}{\partial x} = 0, \tag{33b}$$

$$x = L_c \rightarrow \psi_m = \psi_f. \tag{33c}$$

In Eqs. (32) and (33), β is used to correct the effect of space on the hydraulic diffusivity; L_c is characteristic length of the matrix-block which is half of the matrix-block thickness (h_m). Fig. 1 illustrates a graphical representation of the matrix-fracture system.

3.1. Constant fracture pressure

A solution for the constant fracture pressure is given in our recent work [29]. Since this solution will be used as a basis for the time-dependent boundary condition, the final form of the solution is given in the following. Using an integral method [35–38] the early time solution for constant fracture pressure can be found as follow [29]:

$$\psi_D = \frac{(x_D + \sqrt{24\beta\eta_{D1}t_D} - 1)^3}{24\beta\eta_{D1}t_D\sqrt{24\beta\eta_{D1}t_D}} = \left(1 - \frac{1 - x_D}{\sqrt{24\beta\eta_{D1}t_D}}\right)^3, \quad t_D < \frac{1}{24\beta\eta_{D1}}. \tag{34}$$

$$\bar{\psi}_D = \frac{\sqrt{24\beta\eta_{D1}t_D}}{4}, \quad t_D < \frac{1}{24\beta\eta_{D1}}. \tag{35}$$

where $\bar{\psi}_D$ is the average pseudo-pressure and η_{D1} is hydraulic diffusivity of the fracture in dimensionless form and is expressed as follows:

$$\eta_{D1} = \frac{\eta_m(x_D = 1)}{\bar{\eta}} = \frac{k_m/\mu_f c_f \phi_m}{\bar{\eta}}. \tag{36}$$

The late time solution can be obtained by the method of moments [18,39,40] as given by [29]:

$$\begin{aligned}\psi_D(x_D, t_D) = {} & (1 - 1.252\exp(\beta\lambda_1 t_D) + 0.489\exp(\beta\lambda_2 t_D)) \\ & + (1.793\exp(\beta\lambda_1 t_D) - 6.175\exp(\beta\lambda_2 t_D))x_D^2 \\ & + (-0.541\exp(\beta\lambda_1 t_D) + 5.686\exp(\beta\lambda_2 t_D))x_D^3, \\ & t_D \geqslant \frac{1}{24\beta\eta_{D1}},\end{aligned} \tag{37}$$

$$\bar{\psi}_D = 1 - 0.790\exp(\beta\lambda_1 t_D) - 0.148\exp(\beta\lambda_2 t_D), \quad t_D \geqslant \frac{1}{24\beta\eta_{D1}}, \tag{38}$$

where

$$\lambda_1 = -2.486\eta_{D1}, \tag{39}$$

$$\lambda_2 = -32.181\eta_{D1}. \tag{40}$$

Substituting early and late time average dimensionless pseudo-pressures (Eqs. (35) and (38)) and their derivatives in Eq. (20) leads to the following equation for the dimensionless shape factor for flow of a compressible fluid from a matrix block subject to a constant fracture pressure boundary condition:

$$\sigma h_m^2 = \frac{4\sqrt{6\beta\eta_{D1}}}{\eta_D}\left(\frac{1}{4 - \sqrt{24\beta\eta_{D1}t_D}}\right)\frac{1}{\sqrt{t_D}}, \quad t_D < \frac{1}{24\beta\eta_{D1}} \tag{41}$$

$$\sigma h_m^2 = \frac{4\beta\eta_{D1}}{\eta_D}\frac{1.964\exp(\beta\lambda_1 t_D) + 4.763\exp(\beta\lambda_2 t_D)}{0.790\exp(\beta\lambda_1 t_D) + 0.148\exp(\beta\lambda_2 t_D)}, \quad t_D \geqslant \frac{1}{24\beta\eta_{D1}}. \tag{42}$$

where parameters β and η_D were obtained by matching the early and late time cumulative production from the matrix to the fracture by a numerical flow simulator [41].

3.2. Linearly declining fracture pressure

For the linearly declining fracture pressure the diffusivity equation and its initial and boundary conditions are expressed as follows:

$$\frac{\partial \psi_D}{\partial t_D} = \frac{\partial}{\partial x_D}\left(\beta \eta_D(t) \frac{\partial \psi_D}{\partial x_D}\right), \tag{43}$$

$$t_D = 0 \rightarrow \psi_D = 0, \tag{44a}$$

$$x_D = 0 \rightarrow \frac{\partial \psi_D}{\partial x_D} = 0, \tag{44b}$$

$$x_D = 1 \rightarrow \psi_D = \psi_{fD}(t_D) = \kappa t_D. \tag{44c}$$

For the early time solution of these equations we assume that the trial solution has the following form:

$$\psi_D(x_D, t_D) = \kappa t_D\left(1 - \frac{1 - x_D}{1 - \delta(t_D)}\right)^3. \tag{45}$$

When the boundary condition changes with time the penetration depth in the heat balance integral method (HBIM) is found by solving the following ordinary differential equation [42]:

$$\frac{d}{dt_D}\left[\frac{\psi_{fD}(t_D)\bar{\delta}(t_D)}{n+1} - \frac{\bar{\delta}(t_D)\theta}{(n+1)^2}\right] = \frac{n\psi_{fD}(t_D) + \theta}{\bar{\delta}(t_D)}. \tag{46}$$

In this equation n is the exponent in the trial solution, $n = 3$ for our case, and $\bar{\delta} = 1 - \delta$. In Eq. (46), θ can be found from the following equation [42]:

$$\theta = \frac{\frac{\partial \psi_{fD}}{\partial t_D}\bar{\delta}^2 - n(n-1)\psi_{fD}}{2n - 1}. \tag{47}$$

Solving Eq. (46) for a linearly declining fracture pressure leads to the following penetration depth:

$$\delta \approx 1 - \sqrt{8\beta\eta_{D1}t_D}. \tag{48}$$

It should be noted that Eq. (48) is obtained by assuming $\theta = 0$, in Eq. (46) [42]. If we do not use the assumption of $\theta = 0$, Eq. (46) cannot be solved analytically. The derivation of this equation is shown in Appendix A.1 in more details. Our numerical results show that we can obtain a more accurate solution if we use the following equation for the penetration depth:

$$\delta = 1 - \sqrt{9\beta\eta_{D1}t_D}. \tag{49}$$

The early time solution is valid till the penetration depth reaches the inner boundary, so we can find the time at which the pressure disturbance reaches the boundary (t^*) as follows:

$$0 = 1 - \sqrt{9\beta\eta_{D1}t^*} \Rightarrow t^* = \frac{1}{9\beta\eta_{D1}}. \tag{50}$$

Therefore, the early time solution of the partial differential Eq. (43) with the boundary conditions (44) can be expressed as follows:

$$\psi_D(x_D, t_D) = \kappa t_D\left(1 - \frac{1 - x_D}{\sqrt{9\beta\eta_{D1}t_D}}\right)^3, \quad t_D < \frac{1}{9\beta\eta_{D1}}. \tag{51}$$

Integrating of Eq. (51) over the matrix block volume, leads to Eq. (52) for the early time average dimensionless pseudo pressure:

$$\bar{\psi}_D = \frac{\sqrt{9\beta\eta_{D1}}}{4}kt_D^{3/2}, \quad t_D < \frac{1}{9\beta\eta_{D1}}. \tag{52}$$

The time dependence of the boundary condition for the late time solution can be considered using Duhamel's theorem. When the

fracture pseudo-pressure varies with time (Eq. (44c)), Duhamel's theorem provides the basis to solve the problem with variable boundary conditions based on the solution provided for the constant fracture pseudo-pressure. Using Duhamel's theorem [18,43,44] the solution of PDE (43) with the boundary conditions (44b) and (44c) can be expressed as:

$$\psi_D = \frac{\partial}{\partial t_D}\int_0^{t_D} \psi_{fD}(\tau)\psi_D(x_D, t_D-\tau)d\tau, \tag{53}$$

where ψ_D within the integral is the solution when $\psi_{fD}=1$ and ψ_D on the left-hand side is the solution of PDE (43) when the matrix-fracture boundary condition changes with time.

Using Duhamel's theorem leads to the following late time solution for the case of the linearly declining fracture pressure:

$$\begin{aligned}\psi_D(x_D,t_D) &= \kappa t_D - \frac{0.55790\kappa}{\beta\lambda_1}(2.314-3.314x_D^2+x_D^3)(\exp(\beta\lambda_1 t_D)-1)\\ &\quad + \frac{5.47256\kappa}{\beta\lambda_2}(0.086-1.086x_D^2+x_D^3)(\exp(\beta\lambda_2 t_D)-1),\\ t_D &\geqslant \frac{1}{9\beta\eta_{D1}}.\end{aligned} \tag{54}$$

Derivation of Eq. (54) is shown in Appendix A.1 in more details. The late time average matrix block pseudo-pressure for the linearly declining fracture pressure is obtained as follows:

$$\begin{aligned}\bar{\psi}_D(x_D,t_D) &= \int_0^1 \psi_D dx_D = \kappa t_D - \frac{0.81416\kappa}{\beta\lambda_1}(\exp(\beta\lambda_1 t_D)-1)\\ &\quad - \frac{0.14229\kappa}{\beta\lambda_2}(\exp(\beta\lambda_2 t_D)-1), \quad t_D \geqslant \frac{1}{9\beta\eta_{D1}},\end{aligned} \tag{55}$$

Using the average pseudo-pressure and its derivative in the shape factor equation (Eq. (25)) results in the following equations for the early and late time shape factors in the case of the linearly declining fracture pressure:

$$\sigma h_m^2 = \frac{-3}{2\eta_D}\frac{\sqrt{9\beta\eta_{D1}}}{\left(\frac{\sqrt{9\beta\eta_{D1}}}{4}\sqrt{t_D}-1\right)}\frac{1}{\sqrt{t_D}}, \quad t_D < \frac{1}{9\beta\eta_{D1}}, \tag{56}$$

$$\begin{aligned}\sigma h_m^2 &= \frac{-4\beta\eta_{D1}}{\eta_D}\frac{1-0.81416\exp(\beta\lambda_1 t_D)-0.14229\exp(\beta\lambda_2 t_D)}{0.32750(\exp(\beta\lambda_1 t_D)-1)+0.00442(\exp(\beta\lambda_2 t_D)-1)},\\ t_D &\geqslant \frac{1}{9\beta\eta_{D1}}\end{aligned} \tag{57}$$

It should be noted that for the linearly declining fracture pressure, the shape factor for compressible fluid is not a function of the dimensionless decline constant, κ; a similar observation was reported by Hassanzadeh and Pooladi-Darvish [19] for flow of a slightly compressible fluid in fractured porous media.

3.3. Exponentially declining fracture pressure

For the exponentially declining fracture pressure the solution of the following PDE should be used in Eq. (29) to derive the shape factor for this case:

$$\frac{\partial\psi_D}{\partial t_D} = \frac{\partial}{\partial x_D}\left(\beta\eta_D(t)\frac{\partial\psi_D}{\partial x_D}\right), \tag{58}$$

$$t_D = 0 \rightarrow \psi_D = 0, \tag{59a}$$

$$x_D = 0 \rightarrow \frac{\partial\psi_D}{\partial x_D} = 0, \tag{59b}$$

$$x_D = 1 \rightarrow \psi_D = \psi_{fD}(t_D) = 1-\exp(-\kappa t_D), \tag{59c}$$

The following function is assumed for the early time solution which satisfies the outer boundary condition:

$$\psi_D(x_D,t_D) = (1-\exp(-\kappa t_D))\left(1-\frac{1-x_D}{1-\delta(t_D)}\right)^3. \tag{60}$$

Solving the ODE of Eq. (46) leads to the following equation for the penetration depth in the case of an exponentially declining fracture pressure:

$$\delta \approx 1 - \sqrt{12\beta\eta_{D1}t_D\left(\frac{2}{1-\exp(-\kappa t_D)} - \frac{\sqrt{\pi}}{1-\exp(-\kappa t_D)}\frac{erf(\sqrt{\kappa t_D})}{\sqrt{\kappa t_D}}\right)}. \tag{61}$$

The derivation of this equation is illustrated in Appendix A.2. It should be noted that in Eq. (61), *erf (x)* is the error function defined as follows:

$$erf(\sqrt{\kappa t_D}) = \frac{2}{\sqrt{\pi}}\int_0^{\sqrt{\kappa t_D}} e^{-y^2}dy. \tag{62}$$

Since Eq. (61) is obtained based on an approximation of $\theta=0$ in Eq. (46), our numerical results show that one can obtain a more accurate solution if we use the following equation for penetration depth:

$$\delta = 1 - \sqrt{12.96\beta\eta_{D1}t_D\left(\frac{2}{1-\exp(-\kappa t_D)} - \frac{\sqrt{\pi}}{1-\exp(-\kappa t_D)}\frac{erf(\sqrt{\kappa t_D})}{\sqrt{\kappa t_D}}\right)}. \tag{63}$$

It should be noted that the effect of pressure disturbance will reach the inner boundary when $\delta=0$ and for the exponential decline we cannot obtain an explicit equation for t^* and t^* is determined for any values of k by making Eq. (63) equal to zero. Therefore, the early time solution of Eqs. (58) and (59) can be expressed as follows:

$$\begin{aligned}\psi_D(x_D,t_D) &= (1-\exp(-\kappa t_D))\\ &\quad\times\left(1-\frac{1-x_D}{\sqrt{12.96\beta\eta_{D1}t_D\left(\frac{2}{1-\exp(-\kappa t_D)}-\frac{\sqrt{\pi}}{1-\exp(-\kappa t_D)}\frac{erf(\sqrt{\kappa t_D})}{\sqrt{\kappa t_D}}\right)}}\right)^3,\\ t_D &< t^*.\end{aligned} \tag{64}$$

Integrating of Eq. (64) over the matrix block volume, leads to Eq. (65) for the early time average dimensionless pseudo pressure:

$$\bar{\psi}_D = \frac{\sqrt{1-\exp(-\kappa t_D)}}{4}\times\sqrt{12.96\beta\eta_{D1}t_D\left(2-\frac{\sqrt{\pi}erf(\sqrt{\kappa t_D})}{\sqrt{\kappa t_D}}\right)}, \quad t_D < t^*. \tag{65}$$

Duhamel's theorem and the verified solution of the constant fracture pressure boundary condition lead to the following equation for the late time dimensionless pseudo-pressure in the case of the exponentially declining fracture pressure:

$$\begin{aligned}\psi_D(x_D,t_D) &= 1-\exp(-\kappa t_D) - 0.48743\left(\frac{1-\exp(-\kappa t^*)}{\exp(\beta\lambda_1 t^*)-\exp(-\kappa t^*)}\right)\\ &\quad\times\exp(\beta\lambda_1 t_D)(2.314-3.314x_D^2+x_D^3)\\ &\quad+1.48743\left(\frac{1-\exp(-\kappa t^*)}{\exp(\beta\lambda_2 t^*)-\exp(-\kappa t^*)}\right)\\ &\quad\times\exp(\beta\lambda_2 t_D)(0.086-1.086x_D^2+x_D^3)\\ &\quad+\begin{bmatrix}0.48743\left(\frac{1-\exp(-\kappa t^*)}{\exp(\beta\lambda_1 t^*)-\exp(-\kappa t^*)}\right)(2.314-3.314x_D^2+x_D^3)\\ -1.48743\left(\frac{1-\exp(-\kappa t^*)}{\exp(\beta\lambda_2 t^*)-\exp(-\kappa t^*)}\right)(0.086-1.086x_D^2+x_D^3)\end{bmatrix}\\ &\quad\times\exp(-\kappa t_D), \quad t_D \geqslant t^*.\end{aligned} \tag{66}$$

More details about the derivation of Eq. (66) are discussed in Appendix A.2. Integrating over the matrix-block bulk volume

results in the following equations for the average dimensionless pseudo-pressure in the case of the exponentially declining fracture pressure:

$$\bar{\psi}_D(x_D,t_D)=1-\exp(-\kappa t_D)-0.71132\left(\frac{1-\exp(-\kappa t^*)}{\exp(\beta\lambda_1 t^*)-\exp(-\kappa t^*)}\right)\times\exp(\beta\lambda_1 t_D)-0.03867\left(\frac{1-\exp(-\kappa t^*)}{\exp(\beta\lambda_2 t^*)-\exp(-\kappa t^*)}\right)\times\exp(\beta\lambda_2 t_D)+\left[0.71132\left(\frac{1-\exp(-\kappa t^*)}{\exp(\beta\lambda_1 t^*)-\exp(-\kappa t^*)}\right)+0.03867\left(\frac{1-\exp(-\kappa t^*)}{\exp(\beta\lambda_2 t^*)-\exp(-\kappa t^*)}\right)\right]\exp(-\kappa t_D),\quad t_D\geqslant t^*. \tag{67}$$

Using the average pseudo-pressure and its derivative in Eq. (29) leads to the following equations for the early and late time shape factors in the case of the exponentially declining fracture pressure:

$$\sigma h_m^2=\frac{-1}{\eta_D}\frac{\left\{\begin{array}{l}\frac{\kappa\exp(-\kappa t_D)}{2\sqrt{1-\exp(-\kappa t_D)}}\sqrt{12.96\beta\eta_{D1}t_D\left(2-\sqrt{\pi}\frac{erf(\sqrt{\kappa t_D})}{\sqrt{\kappa t_D}}\right)}+\sqrt{12.96\beta\eta_{D1}(1-\exp(-\kappa t_D))}\\ \times\left[\frac{\left(t_D\left(\frac{-\exp(-\kappa t_D)}{t_D}+\frac{\kappa\sqrt{\pi}erf(\sqrt{\kappa t_D})}{2(\kappa t_D)^{3/2}}\right)+(2-\sqrt{\pi}\frac{erf(\sqrt{\kappa t_D})}{\sqrt{\kappa t_D}})\right)}{2\sqrt{t_D(2-\sqrt{\pi}\frac{erf(\sqrt{\kappa t_D})}{\sqrt{\kappa t_D}})}}\right]\end{array}\right\}}{\frac{\sqrt{1-\exp(-\kappa t_D)}}{4}\sqrt{12.96\beta\eta_{D1}t_D\left(2-\sqrt{\pi}\frac{erf(\sqrt{\kappa t_D})}{\sqrt{\kappa t_D}}\right)}-(1-\exp(-\kappa t_D))},\quad t_D<t^*, \tag{68}$$

$$\sigma h_m^2=\frac{-4}{\eta_D}\frac{\left\{\begin{array}{c}\kappa\exp(-\kappa t_D)\left[1-0.71132\left(\frac{1-\exp(-\kappa t^*)}{\exp(\beta\lambda_1 t^*)-\exp(-\kappa t^*)}\right)-0.03867\left(\frac{1-\exp(-\kappa t^*)}{\exp(\beta\lambda_2 t^*)-\exp(-\kappa t^*)}\right)\right]\\ -0.71132\left(\frac{\beta\lambda_1(1-\exp(-\kappa t^*))}{\exp(\beta\lambda_1 t^*)-\exp(-\kappa t^*)}\right)\exp(\beta\lambda_1 t_D)-0.03867\left(\frac{\beta\lambda_2(1-\exp(-\kappa t^*))}{\exp(\beta\lambda_2 t^*)-\exp(-\kappa t^*)}\right)\exp(\beta\lambda_2 t_D))\end{array}\right\}}{\left\{\begin{array}{c}\left[0.71132\left(\frac{1-\exp(-\kappa t^*)}{\exp(\beta\lambda_1 t^*)-\exp(-\kappa t^*)}\right)+0.03867\left(\frac{1-\exp(-\kappa t^*)}{\exp(\beta\lambda_2 t^*)-\exp(-\kappa t^*)}\right)\right]\exp(-\kappa t_D)\\ -0.71132\left(\frac{1-\exp(-\kappa t^*)}{\exp(\beta\lambda_1 t^*)-\exp(-\kappa t^*)}\right)\exp(\beta\lambda_1 t_D)-0.03867\left(\frac{1-\exp(-\kappa t^*)}{\exp(\beta\lambda_2 t^*)-\exp(-\kappa t^*)}\right)\exp(\beta\lambda_2 t_D)\end{array}\right\}},\quad t_D\geqslant t^* \tag{69}$$

Based on Eqs. (68) and (69), for an exponentially declining fracture pressure the shape factor for a compressible fluid is a function of the decline exponent, k. Similar observations have been made in the previous studies for a slightly compressible fluid [18,19].

4. Model verification

The developed shape factor was validated by a fine-grid single porosity model (Eclipse 100). The total cumulative production from the matrix to the fracture based on the simulator was used to find the correction factor (β) and η_D and to validate the presented model. Fig. 2 shows the matrix-fracture cumulative fluid production *versus* time for a case with $\gamma = 0.7$, $T = 93.3$ °C and pressure drawdown of 45 to 22.5 MPa. The values obtained for the correction factor (β), the matching parameter (η_D), the average hydraulic diffusivity ($\bar{\eta}$) and the dimensionless fracture hydraulic diffusivity (η_{D1}) are 0.730, 0.3127, 0.03457 and 0.3691, respectively. In the model verification studies, a slab-shaped matrix-block with thickness (h_m) of 4 m, permeability of 1mD, and porosity of 0.1 are considered. We use the same reservoir data and parameters throughout this paper. As illustrated in Fig. 2 the approximate analytical model based on this study is in a good agreement with the fine grid numerical simulation. More details about the numerical simulations and more validation cases are discussed elsewhere [29].

The developed model with $\beta = \eta_{D1} = \eta_D = 1$ must reproduce the shape factor for a slightly compressible fluid. For additional validation of the developed model, the shape factor derived here is evaluated with the shape factor of the slightly compressible fluid. Outcomes show that the models developed for different boundary conditions can reproduce the slightly compressible fluid shape factor for the complete period of time.

Fig. 3 compares the developed shape factor model for a slightly compressible fluid ($\beta = \eta_{D1} = \eta_D = 1$) and models available in the literature [18,19] when the fracture pressure declines linearly with time. According to this figure the presented model shows an acceptable match with other models.

Figs. 4–6 demonstrate the comparisons between the presented shape factor models in this study with the literature models for a slightly compressible fluid when the fracture pressure declines exponentially with time for different values of the decline exponent. These figures demonstrate that the presented model can reproduce the slightly compressible fluid shape factor with an acceptable accuracy.

5. Results

In this section a comparison of the developed model with the Warren and Root model [3] is presented and then the behavior of the shape factor for different fracture pressure depletion regimes for flow of a compressible fluid through dual porosity media is described.

5.1. Comparison of model with Warren and Root model

Warren and Root [3] used a pseudo-steady state approach to derive the shape factor for a slightly compressible fluid in the

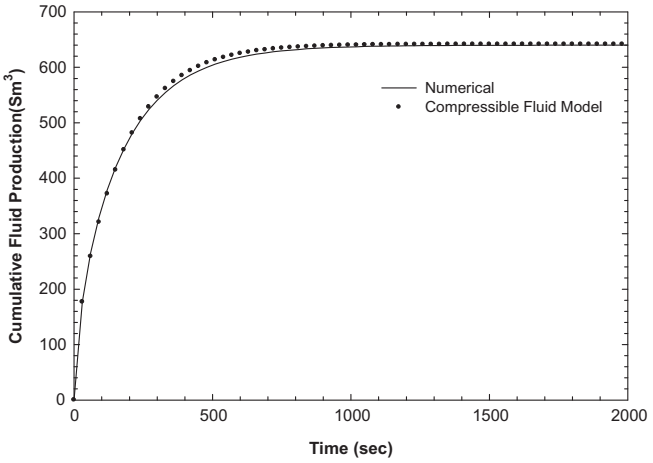

Fig. 2. Comparison of the matrix-fracture cumulative fluid production obtained from the approximate analytical solution and the numerical model of Eclipse for constant fracture pressure.

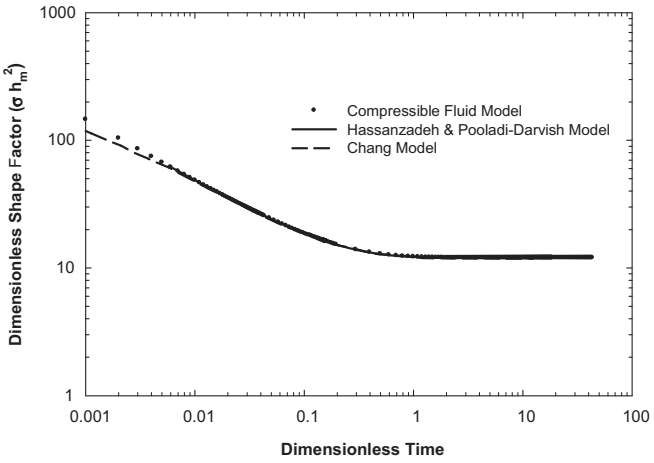

Fig. 3. Comparison of the developed shape factor model with literature models for slightly compressible fluid in the case of linearly declining fracture pressure.

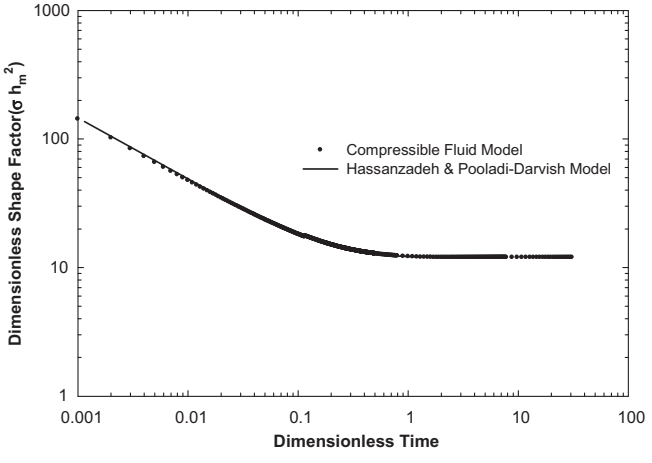

Fig. 4. Comparison of the developed shape factor model with literature models for slightly compressible fluid in the case of exponentially declining fracture pressure for small values of exponent ($k = 0.0001$).

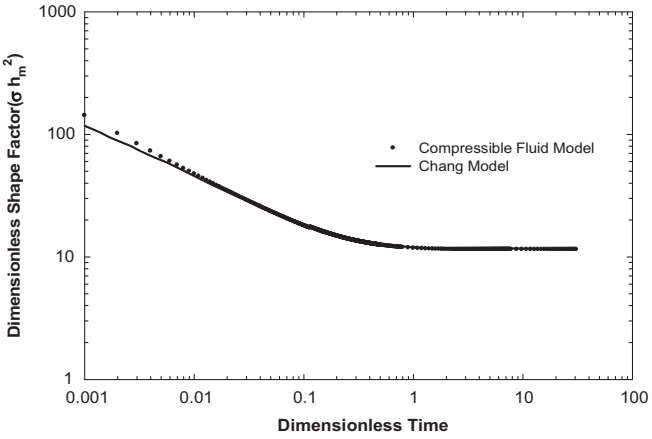

Fig. 5. Comparison of the developed shape factor model with literature models for slightly compressible fluid in the case of exponentially declining fracture pressure ($k = 0.632$).

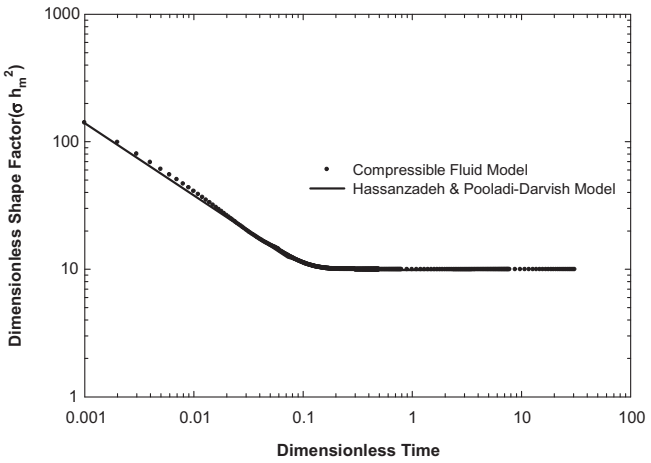

Fig. 6. Comparison of the developed shape factor model with literature models for slightly compressible fluid in the case of exponentially declining fracture pressure for large values of exponent ($k = 1$).

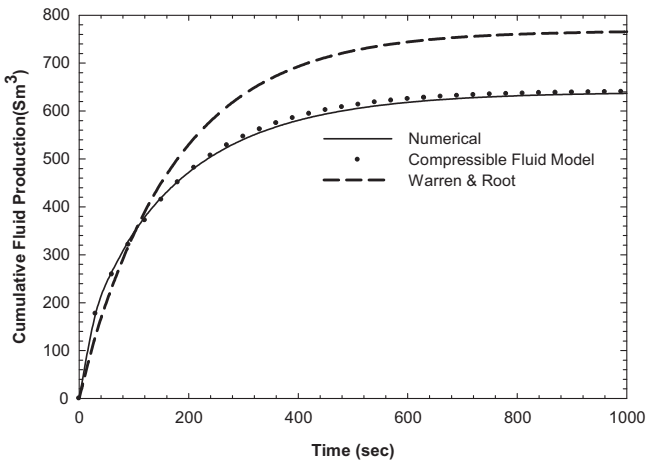

Fig. 7. Comparison of the developed semi-analytical model with numerical and Warren and Root model.

fractured media. They derived the following shape factor for slightly compressible fluid for different sets of fractures,

$$\sigma = \frac{4n(n+1)}{h_m^2}. \tag{70}$$

where n is the number of sets of fractures. For one set of fracture the derived value of the shape factor is $(12/h_m^2)$. Fig. 7 shows the comparison of the matrix-fracture cumulative fluid production based on the Warren and Root shape factor, presented semi-analytical model (time dependent shape factor) and numerical results.

According to Fig. 7 it can be concluded that using a constant slightly compressible fluid shape factor (Based on Warren and Root model) for flow of compressible fluids leads to large error in prediction of the cumulative production from the matrix.

5.2. Linearly declining fracture pressure

Fig. 8 shows the shape factor for the linearly declining fracture pressure derived from Eqs. (56) and (57). The shape factor for a constant fracture pressure is also shown in this figure for comparison. As illustrated in this figure, for the linearly declining fracture pressure, the transient period for the linear decline is longer than that of the constant fracture pressure and the shape factor is stabilized at value of 10.38 when t_D is about 3.81. For the case of the constant fracture pressure the stabilized value of the shape factor is 8.57 when dimensionless time is about 0.7. The same behavior has been reported for a slightly compressible fluid by Chang [18] and Hassanzadeh and Pooladi-Darvish [19] in the case of a slightly compressible fluid. From this figure it can be concluded that the transient and pseudo-steady state values of the shape factor for a linear decline is larger than those of the constant fracture pressure. It should be noted that like slightly compressible fluids, the value of the depletion rate κ has no impact on the transient and stabilized value of the shape factor.

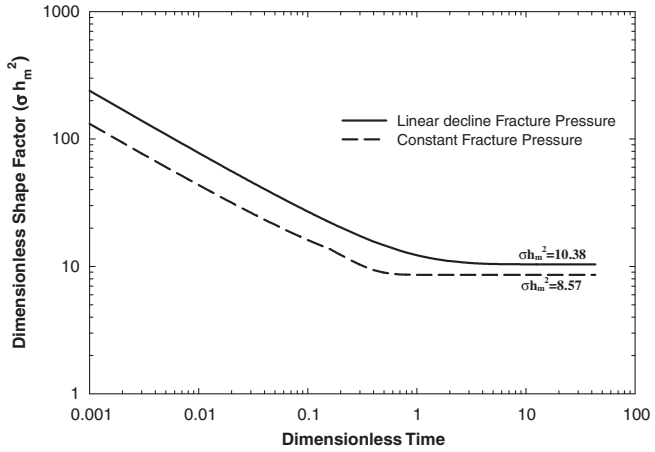

Fig. 8. Comparison of the shape factor for linearly declining and constant fracture pressure.

5.3. Exponentially declining fracture pressure

Fig. 9 shows the effect of the exponent of the exponential decline on the shape factors based on Eqs. (68) and (69). Different values of the decline exponent ranging from 0.0001 to 1,000 are used. A large decline factor implies fast pressure depletion in the fracture while a small value represents a slow depletion. As illustrated in Fig. 9 for small values of κ ($\kappa < 0.1$), the shape factor begins at large values and subsequently converges to a stabilized value of 10.38 as compared to 8.57 for a constant fracture pressure case. As the value of the exponent increases (fast depletion) the transient and pseudo-steady state values of the shape factor tend to those of the constant fracture pressure boundary condition. When $\kappa > 10$ the constant fracture pressure and the exponentially declining fracture pressure have the same value of the stabilized shape factor. Similar behavior was reported for a slightly compressible fluid and exponentially declining fracture pressure by Chang [18] and Hassanzadeh and Pooladi-Darvish [19].

Fig. 10 shows the dimensionless shape factor for flow of a compressible fluid in a dual-porosity medium for various pressure depletion regimes in the fracture. Results show that the stabilized values of the shape factor vary from 8.57 for the constant fracture pressure to 10.38 for the linearly declining fracture pressure. For the exponentially declining fracture pressure the stabilized values vary between these two limits. For a very small value of the exponent (slow depletion) the stabilized value is the same as that for the linearly declining fracture pressure. However, as the value of the exponent increases, the stabilized values of the shape factor for the exponential decline shift to the constant fracture pressure value. At a large value of the exponential decline (fast depletion), the constant and exponentially declining fracture pressures have the same stabilized value of 8.57 for the shape factor.

The above results show that both the transient and pseudo-steady state values of the single-phase shape factor depend on

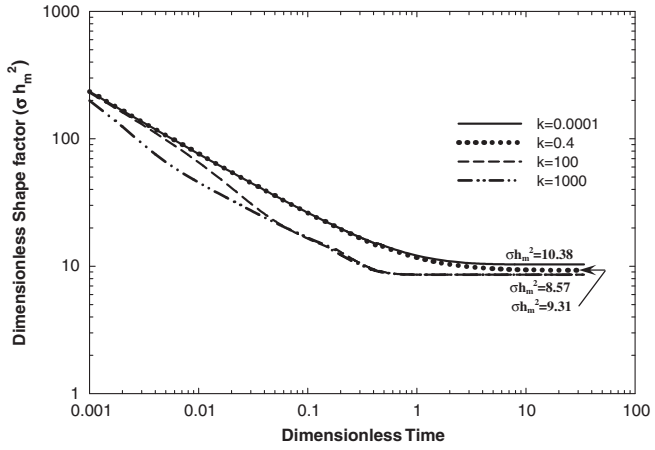

Fig. 9. Shape factor comparison for different exponents for exponentially declining fracture pressure.

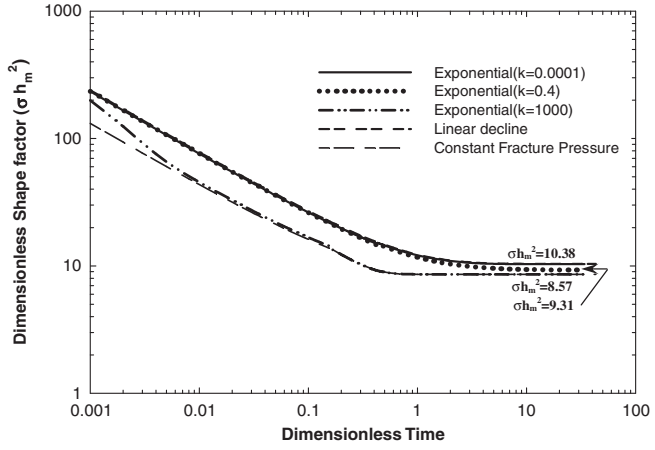

Fig. 10. Comparison of the dimensionless shape factor for different pressure depletion regime in the fracture.

Table 1
Stabilized values of the shape factor and time at which the pressure disturbance reaches the inner boundary for different depletion regimes in the fracture.

Depletion regime in the fracture	t^*	Stabilized value of the dimensionless shape factor
Linear decline	0.412	10.38
Exponential decline (k = 0.0001)	0.429	10.38
Exponential decline (k = 0.4)	0.416	9.31
Exponential decline (k = 1000)	0.154	8.57
Constant fracture pressure	0.155	8.57

how the fracture pressure changes with time. It should be noted for a linearly declining fracture pressure the stabilized value of the shape factor is independent of the decline rate. On the other hand, for an exponential decline the stabilized value of the shape factor depends on the decline exponent. Furthermore, the time dependence of the fracture boundary condition on the stabilized value of the shape factor can be described by using an exponentially declining regime with different decline exponents. In such cases, the small decline exponents replicate the linear pressure decline in the fracture whereas a large decline exponent reproduces the constant fracture pressure boundary condition.

Table 1 shows the stabilized values of the single-phase shape factor and the time at which the effect of pressure disturbance reaches the inner boundary (t^*) for different pressure depletion regimes in the fracture. It should be pointed out that the developed model is applicable for single-phase flow of a compressible fluid in the fractured media.

6. Conclusions

The following major conclusions are made as a result of this study:

- The matrix-fracture shape factor for single-phase flow of compressible fluids illustrates a transient period and then stabilizes to a stable value throughout pseudo-steady state transfer.
- The presented approximate analytical solution revealed that the matrix-fracture transfer shape factor for single phase flow of a compressible fluid in the dual-porosity media is a function of the pressure depletion regime in the fracture.
- Based on the pressure depletion regime in the fracture the stabilized value of the shape factor varies between two limits. The upper limit is obtained for a linearly declining fracture pressure which corresponds to a slow pressure depletion regime. The lower limit is derived for the constant fracture pressure boundary conditions where depletion takes place faster.
- When the fracture pressure depletes exponentially with time, the stabilized value of the shape factor falls between those values of the constant fracture pressure and linearly declining fracture pressure. This stabilized value is a function of the exponent κ. For small exponent values the stabilized shape factor has the same value as that for the linearly declining fracture pressure. For large exponent values, the stabilized value of the shape factor is equal to that for a constant fracture pressure.
- The pseudo-steady state time (stabilization time) of the shape factor increases as the fracture boundary condition changes from a fast depletion regime toward a slow depletion regime.

Acknowledgements

The authors are grateful to Dr. Mehran Pooladi-Darvish (Fekete Associates Inc. and The University of Calgary) for helpful discussions. Financial support of NSERC/AERI/Foundation CMG and iCORE Chairs Funds is acknowledged.

Appendix A. Solution of the gas diffusivity equation for different fracture depletion conditions

A.1. Linearly declining fracture pressure

In this case the following PDE with initial and boundary conditions (Eqs. A1.2a, A1.2b, A1.2c) should be solved:

$$\frac{\partial \psi_D}{\partial t_D} = \frac{\partial}{\partial x_D}\left(\beta \eta_D(t) \frac{\partial \psi_D}{\partial x_D}\right), \tag{A1.1}$$

$$t_D = 0 \rightarrow \psi_D = 0, \tag{A1.2a}$$

$$x_D = 0 \rightarrow \frac{\partial \psi_D}{\partial x_D} = 0, \tag{A1.2b}$$

$$x_D = 1 \rightarrow \psi_D = \psi_{fD}(t_D) = \kappa t_D. \tag{A1.2c}$$

For the early time solution we use the following trial solution:

$$\psi_D(x_D, t_D) = \kappa t_D \left(1 - \frac{1 - x_D}{1 - \delta(t_D)}\right)^3, \tag{A1.3}$$

when the boundary condition changes with time the penetration depth in the heat balance integral method (HBIM) is found by solving the following ordinary differential equation [42]:

$$\frac{d}{dt_D}\left[\frac{\psi_{fD}(t_D)\bar{\delta}(t_D)}{n+1} - \frac{\bar{\delta}(t_D)\theta}{(n+1)^2}\right] = \frac{n\psi_{fD}(t_D) + \theta}{\bar{\delta}(t_D)}. \tag{A1.4}$$

In this equation n is the exponent in the trial solution (n = 3 for our case) and $\bar{\delta} = 1 - \delta$. In Eq. (A1.4), θ can be obtained by using the following equation:

$$\theta = \frac{\frac{\partial \psi_{fD}}{\partial t_D}\bar{\delta}^2 - n(n-1)\psi_{fD}}{2n-1}. \tag{A1.5}$$

Assume that $\bar{\delta} = \varepsilon\sqrt{t_D}$ and substituting this equation in the ODE equation of (A1.4) leads to following ODE for the linearly declining fracture pressure:

$$d\left[\frac{\kappa t_D \varepsilon \sqrt{t_D}}{n+1} - 0\right] = \frac{n\kappa t_D}{\varepsilon\sqrt{t_D}} dt_D. \tag{A1.6}$$

It should be noted that this ODE is obtained by assuming θ = 0 in Eq. (A1.4) [42]. Integrating of Eq. (A1.6) leads to the following equation for ε:

$$\varepsilon = \sqrt{\frac{2n(n+1)}{3}} \overset{n=3}{\rightarrow} \varepsilon = \sqrt{8}. \tag{A1.7}$$

So we reach the following equation for penetration depth in the case of a linear PDE:

$$\bar{\delta} = \varepsilon\sqrt{t_D} = \sqrt{8t_D} \Rightarrow \delta \approx 1 - \sqrt{8t_D}. \tag{A1.8}$$

In the case of a nonlinear PDE we have the following equation for the penetration depth:

$$\delta \approx 1 - \sqrt{8\beta\eta_{D1}t_D}. \tag{A1.9}$$

As was illustrated in the model verification section we can obtain a more accurate solution if we use the following equation for the penetration depth:

$$\delta = 1 - \sqrt{9\beta\eta_{D1}t_D}. \tag{A1.10}$$

Therefore, the early time solution of the partial differential Eq. (A1.1) with the boundary conditions (A1.2) can be expressed as follows:

$$\psi_D(x_D,t_D)=\kappa t_D\left(1-\frac{1-x_D}{\sqrt{9\beta\eta_{D1}t_D}}\right)^3,\quad t_D<\frac{1}{9\beta\eta_{D1}}. \tag{A1.11}$$

Integrating of Eq. (A1.11) over the matrix block volume, leads to the following equation for the early time average dimensionless pseudo pressure:

$$\bar{\psi}_D=\frac{\sqrt{9\beta\eta_{D1}}}{4}kt_D^{3/2},\quad t_D<\frac{1}{9\beta\eta_{D1}}. \tag{A1.12}$$

For the late time solution in the case of the linearly declining fracture pressure the following PDE should be solved. It should be noted that the initial condition for the late time solution comes from the early time solution (Eq. (A1.11)).

$$\frac{\partial\psi_D}{\partial t_D}=\frac{\partial}{\partial x_D}\left(\beta\eta_D(t)\frac{\partial\psi_D}{\partial x_D}\right), \tag{A1.13}$$

$$t_D=\frac{1}{9\beta\eta_{D1}}\rightarrow\psi_D=\left(\frac{\kappa}{9\beta\eta_{D1}}\right)x_D^3, \tag{A1.14a}$$

$$x_D=0\rightarrow\frac{\partial\psi_D}{\partial x_D}=0, \tag{A1.14b}$$

$$x_D=1\rightarrow\psi_D=\psi_{fD}(t_D)=\kappa t_D. \tag{A1.14c}$$

The time dependence of the boundary condition for the late time solution can be considered by Duhamel's theorem. When the fracture pseudo-pressure varies with time (Eq. (A1.14c)), Duhamel's theorem provides the basis to solve the problem with variable boundary conditions based on the solution provided for the constant fracture pseudo-pressure. Using Duhamel's theorem [18,43,44] the solution of PDE (A1.13) with conditions (A1.14) can be expressed as:

$$\psi_D=\frac{\partial}{\partial t_D}\int_0^{t_D}\psi_{fD}(\tau)\psi_D(x_D,t_D-\tau)d\tau,\quad t_D\geqslant\frac{1}{9\beta\eta_{D1}}. \tag{A1.15}$$

In this equation, ψ_D within the integral is the solution when $\psi_{fD}=1$ (Eq. (A1.16)) and ψ_D on the left-hand side is the solution of the PDE when the matrix-fracture boundary condition changes with time.

$$\begin{aligned}\psi_D(x_D,t_D)&=(1+2.314m_1\exp(\beta\lambda_1t_D)+0.086m_2\exp(\beta\lambda_2t_D))\\&+(-3.314m_1\exp(\beta\lambda_1t_D)-1.086m_2\exp(\beta\lambda_2t_D))x_D^2\\&+(m_1\exp(\beta\lambda_1t_D)+m_2\exp(\beta\lambda_2t_D))x_D^3.\end{aligned} \tag{A1.16}$$

Derivation of Eq. (A1.16) has been shown in our previous study [29]. Using Duhamel's theorem and substituting Eqs. (A1.16) and (A1.14c) in Eq. (A1.15) lead to the following late time solution for the case of the linearly declining fracture pressure:

$$\begin{aligned}\psi_D(x_D,t_D)&=\kappa t_D+\left\{\frac{2.314\kappa m_1}{\beta\lambda_1}(\exp(\beta\lambda_1t_D)-1)+\frac{0.086\kappa m_2}{\beta\lambda_2}(\exp(\beta\lambda_2t_D)-1)\right\}\\&-\left\{\overbrace{\frac{3.314\kappa m_1}{\beta\lambda_1}(\exp(\beta\lambda_1t_D)-1)+\frac{1.086\kappa m_2}{\beta\lambda_2}(\exp(\beta\lambda_2t_D)-1)}^{C}\right\}x_D^2\\&+\left\{\overbrace{\frac{\kappa m_1}{\beta\lambda_1}(\exp(\beta\lambda_1t_D)-1)+\frac{\kappa m_2}{\beta\lambda_2}(\exp(\beta\lambda_2t_D)-1)}^{D}\right\}x_D^3,\quad t_D\geqslant\frac{1}{9\beta\eta_{D1}}.\end{aligned} \tag{A1.17}$$

The initial condition is used to find m_1 and m_2 as follows:

$$t_D=t^*=\frac{1}{9\beta\eta_{D1}}\rightarrow C=0,\quad D=\frac{\kappa}{9\beta\eta_{D1}}. \tag{A1.18}$$

Solving the system of Eq. (A1.18) leads to the following values for m_1 and m_2

$$m_1=-0.55790,\quad m_2=5.47256. \tag{A1.19}$$

Using these values in Eq. (A1.17) and some simplifications leads to the following late time pseudo pressure for the linearly declining fracture pressure:

$$\begin{aligned}\psi_D(x_D,t_D)&=\kappa t_D-\frac{0.55790\kappa}{\beta\lambda_1}(2.314-3.314x_D^2+x_D^3)(\exp(\beta\lambda_1t_D)-1)\\&+\frac{5.47256\kappa}{\beta\lambda_2}(0.086-1.086x_D^2+x_D^3)(\exp(\beta\lambda_2t_D)-1),\\t_D&\geqslant\frac{1}{9\beta\eta_{D1}}.\end{aligned} \tag{A1.20}$$

The late time average matrix block pseudo-pressure for the linearly declining fracture pressure is obtained as follows:

$$\begin{aligned}\bar{\psi}_D(x_D,t_D)&=\int_0^1\psi_Ddx_D\\&=\kappa t_D-\frac{0.81416\kappa}{\beta\lambda_1}(\exp(\beta\lambda_1t_D)-1)\\&-\frac{0.14229\kappa}{\beta\lambda_2}(\exp(\beta\lambda_2t_D)-1),\quad t_D\geqslant\frac{1}{9\beta\eta_{D1}}.\end{aligned} \tag{A1.21}$$

A.2. Exponentially declining fracture pressure

When the fracture pressure changes exponentially with time we have the following PDE with these initial and boundary conditions:

$$\frac{\partial\psi_D}{\partial t_D}=\frac{\partial}{\partial x_D}\left(\beta\eta_D(t)\frac{\partial\psi_D}{\partial x_D}\right), \tag{A2.1}$$

$$t_D=0\rightarrow\psi_D=0, \tag{A2.2a}$$

$$x_D=0\rightarrow\frac{\partial\psi_D}{\partial x_D}=0, \tag{A2.2b}$$

$$x_D=1\rightarrow\psi_D=\psi_{fD}(t_D)=1-\exp(-\kappa t_D). \tag{A2.2c}$$

For the early time solution the following trial solution is suggested which satisfies the outer boundary condition:

$$\psi_D(x_D,t_D)=(1-\exp(-\kappa t_D))\left(1-\frac{1-x_D}{1-\delta}\right)^3,\quad t_D<t^*, \tag{A2.3}$$

when the boundary condition change with time, the penetration depth is found by solving the following ODE [42]:

$$\frac{d}{dt_D}\left[\frac{\psi_{fD}(t_D)\bar{\delta}(t_D)}{n+1}-\frac{\bar{\delta}(t_D)\theta}{(n+1)^2}\right]=\frac{n\psi_{fD}(t_D)+\theta}{\bar{\delta}(t_D)}, \tag{A2.4}$$

where:

$$\theta=\frac{\frac{\partial\psi_{fD}}{\partial t_D}\bar{\delta}^2-n(n-1)\psi_{fD}}{2n-1}. \tag{A2.5}$$

By assuming $\theta=0$ and $\bar{\delta}=\varepsilon\sqrt{t_D}$ and substituting Eq. (A2.2c) in (A2.4) we reach the following ODE:

$$d\left[\frac{\varepsilon\sqrt{t_D}(1-\exp(-\kappa t_D))}{n+1}\right]=\frac{n}{\varepsilon}\frac{(1-\exp(-\kappa t_D))}{\sqrt{t_D}}. \tag{A2.6}$$

Solving this ODE for ε, substituting it in the penetration depth equation and taking $n=3$ lead to the following equation for the penetration depth for the linear partial differential equation:

$$\delta\approx1-\sqrt{12t_D\left(\frac{2}{1-\exp(-\kappa t_D)}-\frac{\sqrt{\pi}}{1-\exp(-\kappa t_D)}\frac{erf(\sqrt{\kappa t_D})}{\sqrt{\kappa t_D}}\right)}. \tag{A2.7}$$

And for the nonlinear partial differential equation (Eqs. (A2.1) and (A2.2)) we reach to the following equation for the penetration depth:

$$\delta \approx 1-\sqrt{12\beta\eta_{D1}t_D\left(\frac{2}{1-\exp(-\kappa t_D)}-\frac{\sqrt{\pi}}{1-\exp(-\kappa t_D)}\frac{erf(\sqrt{\kappa t_D})}{\sqrt{\kappa t_D}}\right)}. \tag{A2.8}$$

Our numerical results show that we can increase the accuracy of the solution if we use the following equation for the penetration depth:

$$\delta = 1-\sqrt{12.96\beta\eta_{D1}t_D\left(\frac{2}{1-\exp(-\kappa t_D)}-\frac{\sqrt{\pi}}{1-\exp(-\kappa t_D)}\frac{erf(\sqrt{\kappa t_D})}{\sqrt{\kappa t_D}}\right)}. \tag{A2.9}$$

Therefore, the early time solution in Eqs. (A2.1) and (A2.2) can be expressed as follows:

$$\psi_D(x_D,t_D) = (1-\exp(-\kappa t_D)) \times\left(1-\frac{1-x_D}{\sqrt{12.96\beta\eta_{D1}t_D\left(\frac{2}{1-\exp(-\kappa t_D)}-\frac{\sqrt{\pi}}{1-\exp(-\kappa t_D)}\frac{erf(\sqrt{\kappa t_D})}{\sqrt{\kappa t_D}}\right)}}\right)^3, \quad t_D < t^*. \tag{A2.10}$$

Integrating of Eq. (A2.10) over the matrix block volume, leads to the following equation for the early time average dimensionless pseudo pressure:

$$\bar{\psi}_D = \frac{\sqrt{1-\exp(-\kappa t_D)}}{4}\sqrt{12.96\beta\eta_{D1}t_D\left(2-\frac{\sqrt{\pi}erf(\sqrt{\kappa t_D})}{\sqrt{\kappa t_D}}\right)}, \quad t_D < t^*. \tag{A2.11}$$

For the late time solution in the case of the exponentially declining fracture pressure the following PDE should be solved. It should be noted that the initial condition for the late time solution comes from the early time solution (Eq. (A2.10)).

$$\frac{\partial\psi_D}{\partial t_D} = \frac{\partial}{\partial x_D}\left(\beta\eta_D(t)\frac{\partial\psi_D}{\partial x_D}\right), \tag{A2.12}$$

$$t_D = t^* \rightarrow \psi_D = (1-\exp(-\kappa t^*))x_D^3, \tag{A2.13a}$$

$$x_D = 0 \rightarrow \frac{\partial\psi_D}{\partial x_D} = 0, \tag{A2.13b}$$

$$x_D = 1 \rightarrow \psi_D = \psi_{fD}(t_D) = 1-\exp(-\kappa t_D). \tag{A2.13c}$$

Using Duhamel's theorem (Eq. (A1.15)) and the solution of the constant fracture pressure (Eq. (A1.16)) leads to the following late time solution for the case of the exponentially declining fracture pressure:

$$\begin{aligned}\psi_D(x_D,t_D) &= 1-\exp(-\kappa t_D)\\ &+\left\{\begin{array}{l} 2.314m_1\left(1-\frac{\beta\lambda_1}{\kappa+\beta\lambda_1}\right)\exp(\beta\lambda_1 t_D)+0.086m_2\left(1-\frac{\beta\lambda_2}{\kappa+\beta\lambda_2}\right)\exp(\beta\lambda_2 t_D)\\ -\left(\frac{2.314\kappa m_1}{\kappa+\beta\lambda_1}+\frac{0.086\kappa m_2}{\kappa+\beta\lambda_2}\right)\exp(-\kappa t_D)\end{array}\right\}\\ &-\left\{\begin{array}{l}\overbrace{3.314m_1\left(1-\frac{\beta\lambda_1}{\kappa+\beta\lambda_1}\right)\exp(\beta\lambda_1 t_D)+1.086m_2\left(1-\frac{\beta\lambda_2}{\kappa+\beta\lambda_2}\right)\exp(\beta\lambda_2 t_D)}^{C}\\ \underbrace{-\left(\frac{3.314\kappa m_1}{\kappa+\beta\lambda_1}+\frac{1.086\kappa m_2}{\kappa+\beta\lambda_2}\right)\exp(-\kappa t_D)}_{C}\end{array}\right\}x_D^2\\ &+\left\{\begin{array}{l}\overbrace{m_1\left(1-\frac{\beta\lambda_1}{\kappa+\beta\lambda_1}\right)\exp(\beta\lambda_1 t_D)+m_2\left(1-\frac{\beta\lambda_2}{\kappa+\beta\lambda_2}\right)\exp(\beta\lambda_2 t_D)}^{D}\\ \underbrace{-\left(\frac{\kappa m_1}{\kappa+\beta\lambda_1}+\frac{\kappa m_2}{\kappa+\beta\lambda_2}\right)\exp(-\kappa t_D)}_{D}\end{array}\right\}x_D^3, \quad t_D \geqslant t^*.\end{aligned} \tag{A2.14}$$

The initial condition is used to find m_1 and m_2 as follows:

$$t_D = t^* \rightarrow C = 0, \quad D = 1-\exp(-\kappa t^*). \tag{A2.15}$$

Solving the system of Eq. (A2.15) leads to the following values for m_1 and m_2

$$\begin{cases} m_1 = -0.48743\frac{\kappa+\beta\lambda_1}{\kappa}\frac{1-\exp(-\kappa t^*)}{\exp(\beta\lambda_1 t^*)-\exp(-\kappa t^*)},\\ m_2 = 1.48743\frac{\kappa+\beta\lambda_2}{\kappa}\frac{1-\exp(-\kappa t^*)}{\exp(\beta\lambda_2 t^*)-\exp(-\kappa t^*)}.\end{cases} \tag{A2.16}$$

Using these values in Eq. (A2.14) and simplifying lead to the following late time pseudo pressure for the exponentially declining fracture pressure:

$$\begin{aligned}\psi_D(x_D,t_D) &= 1-\exp(-\kappa t_D)-0.48743\left(\frac{1-e^{-\kappa t^*}}{e^{\beta\lambda_1 t^*}-e^{-\kappa t^*}}\right)\\ &\times\exp(\beta\lambda_1 t_D)(2.314-3.314x_D^2+x_D^3)\\ &+1.48743\left(\frac{1-e^{-\kappa t^*}}{e^{\beta\lambda_2 t^*}-e^{-\kappa t^*}}\right)\exp(\beta\lambda_2 t_D)(0.086-1.086x_D^2+x_D^3)\\ &+\left[\begin{array}{l}0.48743\left(\frac{1-e^{-\kappa t^*}}{e^{\beta\lambda_1 t^*}-e^{-\kappa t^*}}\right)(2.314-3.314x_D^2+x_D^3)-\\ 1.48743\left(\frac{1-e^{-\kappa t^*}}{e^{\beta\lambda_2 t^*}-e^{-\kappa t^*}}\right)(0.086-1.086x_D^2+1x_D^3)\end{array}\right]\exp(-\kappa t_D),\\ t_D &\geqslant t^*.\end{aligned} \tag{A2.17}$$

Integrating over the matrix block volume results in the following equations for the average dimensionless pseudo-pressure in the case of the exponentially declining fracture pressure:

$$\begin{aligned}\bar{\psi}_D(x_D,t_D) &= 1-\exp(-\kappa t_D)-0.71132\left(\frac{1-e^{-\kappa t^*}}{e^{\beta\lambda_1 t^*}-e^{-\kappa t^*}}\right)\exp(\beta\lambda_1 t_D)\\ &-0.03867\left(\frac{1-e^{-\kappa t^*}}{e^{\beta\lambda_2 t^*}-e^{-\kappa t^*}}\right)\exp(\beta\lambda_2 t_D)\\ &+\left(0.71132\left(\frac{1-e^{-\kappa t^*}}{e^{\beta\lambda_2 t^*}-e^{-\kappa t^*}}\right)+0.03867\left(\frac{1-e^{-\kappa t^*}}{e^{\beta\lambda_2 t^*}-e^{-\kappa t^*}}\right)\right)\\ &\times\exp(-\kappa t_D), \quad t_D \geqslant t^*.\end{aligned} \tag{A2.18}$$

References

[1] Deng H, Dai Z, Wolfsberg A, Lu Z, Ye M, Reimus P. Upscaling of reactive mass transport in fractured rocks with multimodal reactive mineral facies. Water Resour Res 2010;46:W06501. doi:10.1029/2009WR008363.

[2] Chen ZX. Transient flow of slightly compressible fluids through double-porosity, double-permeability systems-a state-of-the-art review. Transp Porous Med 1989;4:147–84.

[3] Warren JE, Root PJ. The behavior of naturally fractured reservoirs. Soc Pet Eng J 1963:245–55.

[4] Beckner BL. Improved modeling of imbibition matrix/fracture fluid transfer in double porosity simulators. Ph.D. dissertation, Stanford University, 1990.

[5] Cihan A, Tyner JS. 2-D radial analytical solutions for solute transport in a dual-porosity medium. Water Resour Res 2010;doi: 10.1029/2009WR008969, in press.

[6] Di Donato G, Blunt MJ. Streamline-based dual-porosity simulation of reactive transport and flow in fractured reservoirs. Water Resour Res 2004;40:W04203. doi:10.1029/2003WR002772.

[7] Liu MX, Chen ZX. Exact solution for flow of slightly compressible fluids through multiple-porosity, multiple-permeability media. Water Resour Res 1990;26(7):1393–400.

[8] Zimmerman RW, Hadgu T, Bodvarsson GS. A new lumped-parameter model for flow in unsaturated dual-porosity media. Adv Water Res 1996;19(5):317–27.

[9] Kazemi H, Gilman JR. Multiphase flow in fractured petroleum reservoirs. In: Bear J, Tsang CF, de Marsily G, editors. Flow and contaminant transport in fractured rock. San Diego: Academic Press; 1993. p. 267–323.

[10] Bourbiaux B, Granet S, Landereau P, Noetinger B, Sarda S, Sabathier JC. Scaling up matrix-fracture transfer in dual-porosity models: theory and application. SPE Paper 56557, 10.2118/56557-MS, 1999.

[11] Coats KH. Implicit compositional simulation of single-porosity and dual-porosity reservoirs. SPE paper 18427, 10.2118/18427-MS, 1989.

[12] Kazemi H, Merrill LS, Porterfield KL, Zeman PR. Numerical simulation of water-oil flow in naturally fractured reservoirs. Soc Pet Eng J 1976:317–26.

[13] Quintard M, Whitaker S. Transport in chemically and mechanically heterogeneous porous media. I: theoretical development of region-averaged equations for slightly compressible single-phase flow. Adv Water Res 1996;19(1):29–47.

[14] Quintard M, Whitaker S. Transport in chemically and mechanically heterogeneous porous media II: comparison with numerical experiments for slightly compressible single-phase flow. Adv Water Res 1996;19:49–60.

[15] Quintard M, Whitaker S. Transport in chemically and mechanically heterogeneous porous media III: Large-scale mechanical equilibrium and the regional form of Darcy's law. Adv Water Res 1998;21(7):617–29.

[16] Thomas LK, Dixon TN, Pierson RG. Fractured reservoir simulation. Soc Pet Eng J 1983:42–54.

[17] Ueda Y, Murata S, Watanabe Y, Fanatsu K. Investigation of the shape factor used in the dual-porosity reservoir simulator. SPE paper 19469, doi:10.2118/19469-MS; 1989.

[18] Chang MM. Analytical solution to single and two-phase flow problems of naturally fractured reservoirs: theoretical shape factor and transfer functions. Ph.D. dissertation, The University of Tulsa; 1995.

[19] Hassanzadeh H, Pooladi-Darvish M. Effects of fracture boundary conditions on matrix-fracture transfer shape factor. Transp Porous Med 2006;64:51–71.

[20] Lim KT, Aziz K. Matrix-fracture transfer shape factors for dual-porosity simulators. J Pet Sci Eng 1995;13:169–78.

[21] Hassanzadeh H, Pooladi-Darvish M, Atabay S. Shape factor in the drawdown solution for well testing of dual-porosity systems. Adv Water Res 2009;32:1652–63.

[22] Shan C, Pruess K. An analytical solution for slug tracer tests in fractured reservoirs. Water Resour Res 2005;41:W08502. doi:10.1029/2005WR004081.

[23] Zimmerman RW, Chen G, Hadgu T, Bodvarsson GS. A numerical dual-porosity model with semi-analytical treatment of fracture/matrix flow. Water Resour Res 1993;29(7):2127–37.

[24] Rangel-German E, Kavscek AR, Akin S. Time-dependent shape factors for uniform and non-uniform pressure boundary conditions. Transp Porous Med 2010;83:591–601.

[25] Civan F, Rasmussen ML. Analytical hindered-matrix-fracture transfer models for naturally fractured petroleum reservoirs. SPE paper 74364, doi: 10.2118/74364-MS, 2002.

[26] van Heel APG, Boerrigter PM, van Drop JJ. Thermal and hydraulic matrix-fracture interaction in dual permeability simulation. Soc Pet Eng J 2008:735–49.

[27] Lu M, Connel LD. A dual-porosity model for gas reservoir flow incorporating adsorption behavior-part I. Theoretical development and asymptotic analysis. Transp Porous Med 2007;68:153–73.

[28] Penuela G, Civan F, Hughes RG, Wiggins ML. Time-dependent shape factors for interporosity flow in naturally fractured gas-condensate reservoirs. SPE paper 75524; 2002.

[29] Ranjbar E, Hassanzadeh H. Matrix-fracture transfer shape factor for modeling flow of a compressible fluid in dual-porosity media. Adv Water Res 2011;34(5):627–39. doi:10.1016/j.advwatres.2011.02.012.

[30] Hoteit H, Firoozabadi A. Multicomponent fluid flow by discontinuous Galerkin and mixed methods in unfractured and fractured media. Water Resour Res 2005;41:W11412. doi:10.1029/2005WR004339.

[31] Karimi-Fard M, Firoozabadi A. Numerical simulation of water injection in fractured media using the discrete-fracture model and the Galerkin method. Soc Pet Eng J 2003;6(2):117–26.

[32] Lemonnier P, Bourbiaux B. Simulation of naturally fractured reservoirs. State of the art. Part 1: Physical mechanisms and simulator formulations. Oil and Gas Science and Technology 2010;65(2):239–62.

[33] Agarwal RG. Real gas pseudo-time-A new function for pressure build-up analysis of MHF gas wells. SPE paper 8279, 10.2118/8279-MS, 1979.

[34] Ikoku CU. Natural gas reservoir engineering. Florida: Krieger; 1992.

[35] Finlayson BA. The method of weighted residuals and variational principles. New York: Academic Press; 1972.

[36] Goodman TR. Application of integral methods to transient nonlinear heat transfer. Advances in heat transfer, vol. 1. San Diego, CA: Academic; 1964. p. 51-122.

[37] Pooladi-Darvish M, Tortike WS, Farouq Ali SM. Non-isothermal gravity drainage under conduction heating. Petroleum Society of CIM and AOSTRA. Paper NO 94-65, 1994.

[38] Zimmerman RW, Bodvarsson GS. An approximate solution for one-dimensional absorption in unsaturated porous media. Water Resour Res 1989;25(6):1422–8.

[39] Ames WF. Nonlinear partial differential equations in engineering. New York: Academic Press; 1965.

[40] Crank J. The mathematics of diffusion. Oxford: Clarendon Press; 1975.

[41] Geo-Quest. Eclipse 100 technical descriptions 2009.1. Geo-Quest, Schlumberger; 2009.

[42] Mitchel SL, Myers TG. Improving the accuracy of heat balance integral methods applied to thermal problems with time dependent boundary conditions. Int J Heat Mass Transfer 2010;53:3540–51.

[43] Özisik MN. Heat conduction. United States: John Wiley & Sons Inc; 1993.

[44] Polyanin AD. Handbook of linear partial differential equations for engineers and scientists. United States: CRC Press; 2001.